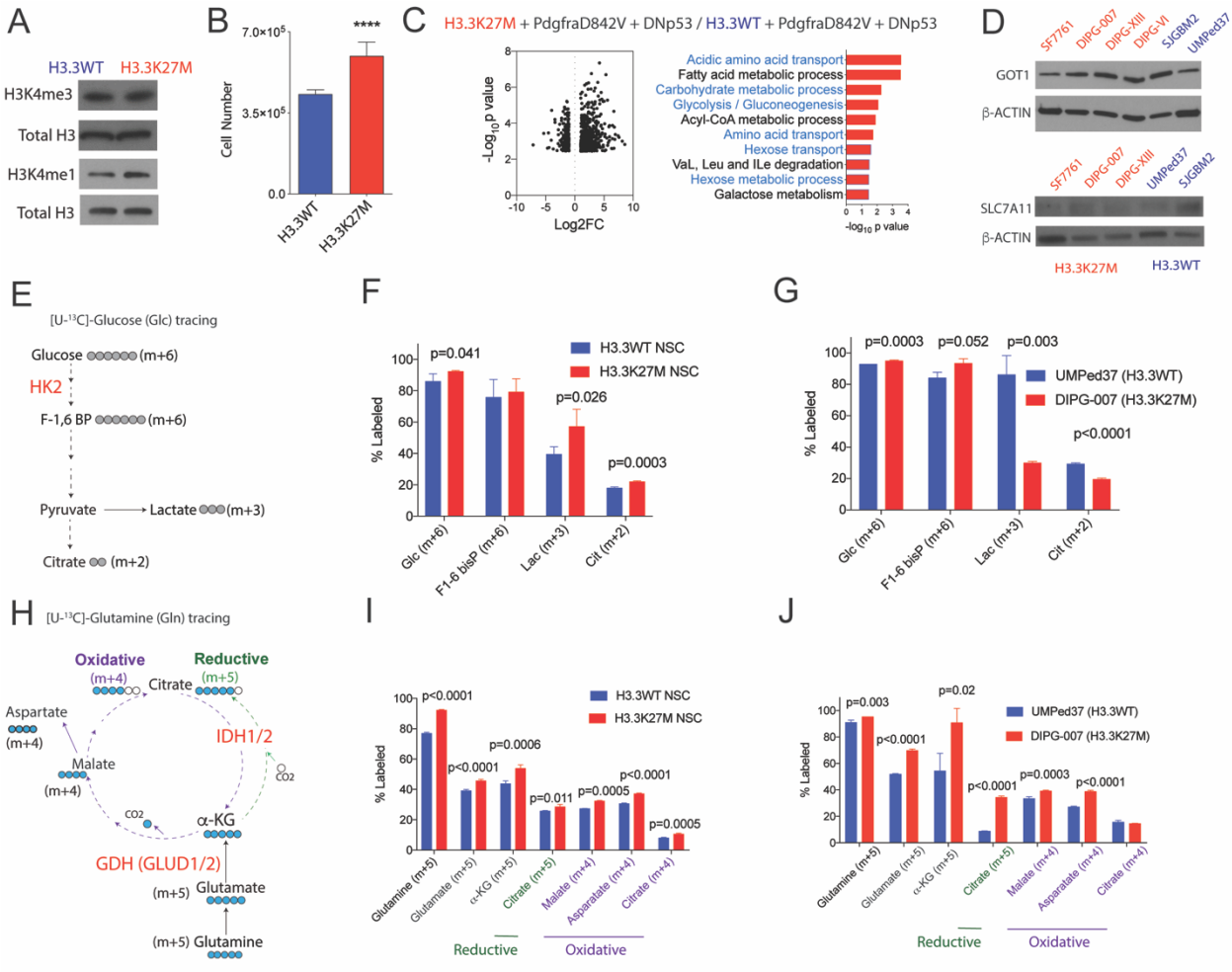

Figure S1. H3.3K27M cells show upregulation of glucose and glutamine metabolism, related to figure 1

(**A**) Representative WB for H3K4me3, H3K4me1 and total H3 in H3.3K27M and H3.3WT NSC.

(**B**) Cell counts in H3.3K27M and H3.3WT NSC after 3 days in culture (n=3, each).

(**C**) Volcano plot and GSEA pathway analysis of metabolic genes upregulated in H3.3K27M, *Pdgfra* D842V, DN*Tp53* versus H3.3WT, *Pdgfra* D842V, DN*Tp53* isogenic mouse cells (n=3, each). Data obtained from (Patel et al., 2019).

(**D**) Representative WB for GOT1 and SLC7A11 in H3.3K27M (SF7761, DIPG-007, DIPG-XIII, red) and H3WT (UMPed37 and SJGBM2, blue) human cell lines. β-ACTIN was used as loading control.

(**E**) Abbreviated schematic of [U-^{13}C]-glucose ([U-^{13}C]-Glc) labeling in glycolysis: with six ^{13}C-labeled carbons (m+6, gray circles), fructose-1,-6-bisphosphate with six ^{13}C-labeled carbons (F-1,6-bisP, m+6), lactate with three ^{13}C-labeled carbons (Lac, m+3) and citrate with two ^{13}C-labeled carbons (Cit, m+2).

(**F-G**) Bar graph demonstrating % labeled metabolites (Y-axis) from the schematic in Figure S1e in H3.3K27M (red) or H3.3WT (blue) NSC (n = 4, each) (**f**), and DIPG-007 (H3.3K27M, red) or UMPed37 (H3WT, blue) (**g**) cells incubated with [U-^{13}C]-Glc (n = 4, each). Note that UMPed37 cells harbor *EGFR* mutations, which are known to enhance glycolysis and lactate production (Guo et al., 2009).

(**H**) Abbreviated schematic of [U-^{13}C]-glutamine ([U-^{13}C]-Gln) labeling in glutaminolysis in relation to the TCA-cycle: with five ^{13}C-labeled carbons in glutamate (Glu) and α-KG (m+5, light blue). Note that Gln-derived citrate can be generated via oxidative decarboxylation (four ^{13}C-labeled carbons; m+4, purple), or reductive carboxylation (five ^{13}C-labeled carbons; m+5, green) pathways.

(**I-J**) Bar graph demonstrating % labeled metabolites (Y-axis) from the schematic in Figure S1h in H3.3K27M (red) or H3.3WT (blue) NSC (n = 4, each) (**i**), and DIPG-007 (H3.3K27M, red) or UMPed37 (H3WT, blue) (**j**) cells incubated with [U-^{13}C]-Gln (n = 4 for all except α-KG, n = 3). Note that H3.3K27M (NSC and DIPG-007) cells show higher citrate levels derived from the reductive carboxylation pathway (five ^{13}C-labeled carbons; m+5, green) compared to H3WT cells (NSC and UMPed37).

Data plotted as mean ± SD and analyzed using 2-sided, unpaired, 2-tailed, Student's t-test; n indicates biologic replicates.

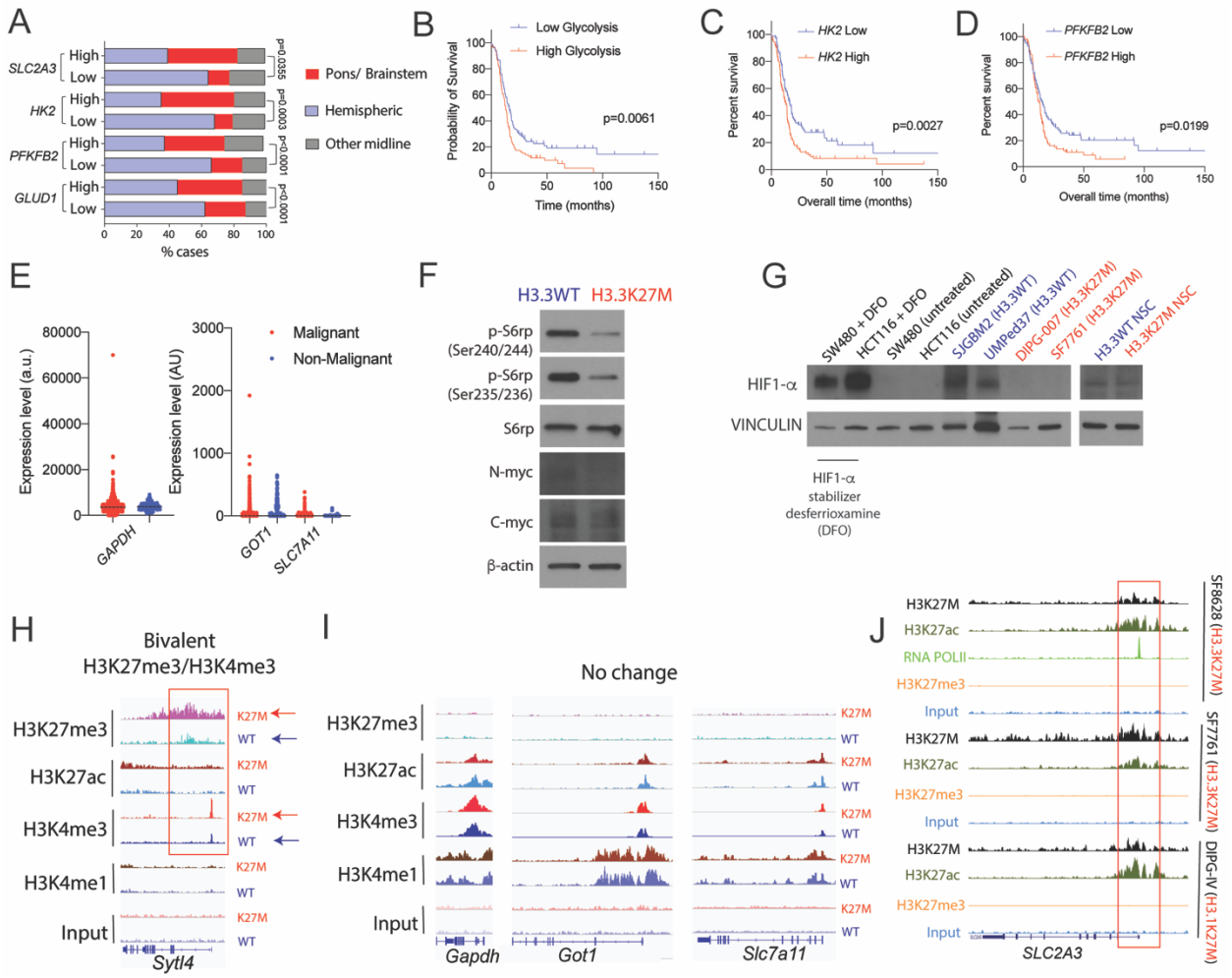

Figure S2. Metabolic enzyme enrichment relates with specific clinical features H3K27M tumors, related to figure 1

(**A**) Bar graph of anatomical location (red, brainstem; light blue, hemispheric; dark gray, other midline) of tumors depicted in **figure 1i** that expressed high (above median) or low (below median) levels of indicated metabolic enzymes. Data analyzed by 2-tailed, Chi square test.

(**B**) We sought to assess if upregulation of glycolytic enzymes is associated with overall prognosis independent of H3K27M status. We determined expression levels of genes in the glycolysis-KEGG (Kyoto Encyclopedia of Genes and Genomes) pathway in pediatric high-grade glioma patients of tumors depicted in **figure 1l** and used unbiased K-means clustering to segregate pediatric high-grade gliomas with high (n=90) versus low (n=98)

glycolytic gene signatures. Log-rank analysis showed a significant difference in overall survival between high *versus* low glycolytic gene expression independent of H3K27M status.

(**C-D**) Log-rank analysis of overall survival in pediatric high-grade glioma patients of tumors depicted in **figure 1I** stratified by high (above median, n=94) or low (below median, n=94) *HK2* (**C**) or *PFKFB2* (**D**) expression.

(**E**) Single cell RNA-seq scatter plot of *GAPDH, GOT1* and *SLC7A11* in H3K27M patient tumor samples. Data derived from (Filbin et al., 2018).

(**F**) Representative WB for p-s6rp (Ser240/244), p-s6rp (Ser235/236) and s6rp (as surrogates for mTor activation) and N-Myc, C-Myc and β-actin in H3.3WT (blue) and H3.3K27M (red) NSC.

(**G**) Representative WB for HIF-1α and VINCULIN in H3WT (SJGBM2, UMPed37 and NSC; blue) and H3.3K27M (DIPG-007, SF7761 and NSC; red) cells. SW480 and HCT116 colon cancer cell lines with or without treatment with the HIF-1α stabilizer desferrioxamine (DFO) were used as controls.

(**H**) Representative IGV genome browser tracks for H3K27me3, H3K27ac, H3K4me3, H3K4me1 and input in H3.3K27M and H3.3WT NSC at *Sytl4* locus demonstrating bivalency (enrichment for both H3K27me3 and H3K4me3, red box) (Larson et al., 2019). For each mark, top panel K27M= H3.3K27M, bottom panel WT=H3.3WT NSC.

(**I**) Representative IGV genome browser tracks for H3K27me3, H3K27ac, H3K4me3, H3K4me1 and input in H3.3K27M and H3.3WT NSC at *Gapdh, Got1* and *Slc7a11* gene loci. For each mark, top panel K27M= H3.3K27M, bottom panel WT=H3.3WT NSC. Note minimal or no difference in enrichment of any of these marks between H3.3K27M and H3.3WT NSC.

(**J**) Representative IGV genome browser tracks for H3K27M, H3K27ac, RNA Pol II and H3K27me3 at *SLC2A3* gene locus in SF8628 (H3.3K27M), SF7761 (H3.3K27M) and DIPG-IV (H3.1K27M) cells. Red boxes indicate overlap in peaks.

Data were analyzed by Log-rank (S2b-d) analysis. Data derived: in S2a-d from PedcBioPortal; S2e from Filbin et al. 2018 (Filbin et al., 2018) and S2j Piunti et al. (Piunti et al., 2017).

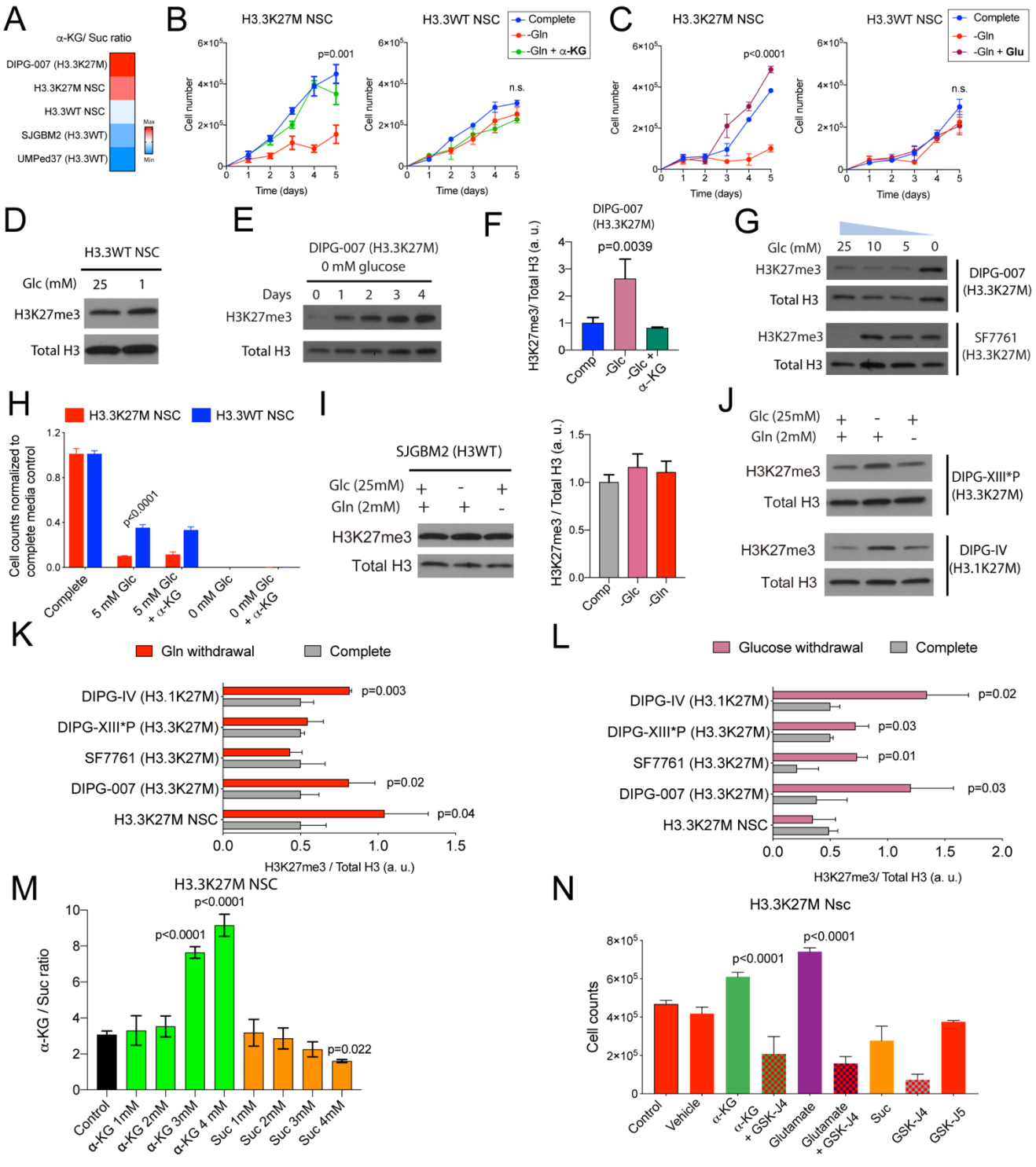

Figure S3. Heterogeneous regulation of global H3K27me3 levels by glutamine and glucose metabolism in H3.3K27M cells, related to figure 3

(**A**) α-KG/Suc ratios in H3.3K27M (DIPG-007 and NSC) and H3WT (NSC, SJGBM2 and UMPed37) cells.

(**B**) Cell counts (Y-axis) over time (days, X-axis) on Gln withdrawal with/without 4 mM cell-permeable α-KG in H3.3K27M or H3.3WT NSC (n = 4, each).

(**C**) Cell counts (Y-axis) over time (days, X-axis) on Gln withdrawal with/without 4 mM cell-permeable glutamate in H3.3K27M or H3.3WT NSC (n = 4, each).

Note that H3K27M, but not H3WT NSC, are sensitive to Gln withdrawal, which was completely rescued by α-KG or glutamate.

(**D**) Representative WB of H3K27me3 and total H3 in H3.3WT NSC cultured in complete or Glc-depleted media for 4 days.

(**E**) Representative WB of H3K27me3 and total H3 in H3.3K27M DIPG-007 cells cultured in Glc-depleted media for indicated days.

(**F**) WB quantification of H3K27me3 normalized to total H3 in DIPG-007 H3.3K27M cells in complete or Glc-depleted media with or without 4 mM cell-permeable α-KG for 4 days (n=3, each).

(**G**) Representative WB of H3K27me3 in H3.3K27M DIPG-007 and SF7761 cells cultured in media at indicated Glc concentration for 4 days.

(**H**) Cell counts normalized to control untreated conditions (Y-axis) on Glc withdrawal with or without 4 mM cell-permeable α-KG in H3.3K27M (red) and H3.3WT (blue) NSC (n = 3, each). Note that H3.3K27M are more sensitive to Glc withdrawal compared to H3.3WT NSC. Cell-permeable α-KG did not rescue cell viability on Glc withdrawal in both cell types.

(**I**) Representative WB of H3K27me3 and quantification normalized to total H3 in H3WT SJGBM2 cells cultured in complete or glucose depleted (pale red) or glutamine depleted (red) media for 4 days (n=3, each).

(**J**) Representative WB of H3K27me3 and quantification normalized to total H3 in DIPG-XIII*P (H3.3K27M) and DIPG-IV (H3.1K27M) cells cultured in complete or glucose depleted or glutamine depleted media for 4 days (n=3, each).

(**K**) Quantification of H3K27me3 normalized to total H3 in H3.1K27M (DIPG-IV, n=3) and H3.3K27M (DIPG-XIII*P, n=3; SF7761, n=4; DIPG-007, n=4; and H3.3K27M NSC, n=3) cell lines cultured in complete or glutamine depleted (red) media for 4 days.

(**L**) Quantification of H3K27me3 normalized to total H3 in H3.1K27M (DIPG-IV, n=3) and H3.3K27M (DIPG-XIII*P, n=3; SF7761, n=4; DIPG-007, n=4; and H3.3K27M NSC, n=3) cell lines cultured in complete or glucose depleted (pale red) media for 4 days.

(**M**) Bar graph demonstrating α-KG/ suc ratios in H3.3K27M DIPG-007 cells treated with indicated concentrations of cell-permeable (dimethyl) α-KG or succinate (n=3, each).

(**N**) Cell counts (Y-axis) on treatment of H3K27M NSC with vehicle, 4 mM cell-permeable α-KG or glutamate with/without the H3K27 demethylase inhibitor GSK-J4, succinate, GSK-J4 alone, or GSK-J5 inactive analogue. Note that succinate lowered while α-KG or glutamate treatment increased H3.3K27M NSC cell numbers. GSK-J4 reversed increased cell proliferation on α-KG or glutamate treatment (n=3).

Cell counts were performed after 4 days in culture. For cell counts, 50,000 cells were plated in 24-well plate. After 4 days of nutrient withdrawal or α-KG or suc treatment, cells were counted and normalized to average complete media cell counts for a given cell type. All WB are representative. Data plotted as mean ± SD and analyzed by 2-sided and analyzed by one-way or two-way ANOVA (S3b-c, g-i, and m-n) or unpaired, 2-tailed, Student's t-test (S3k-l); n indicates biologic replicates.

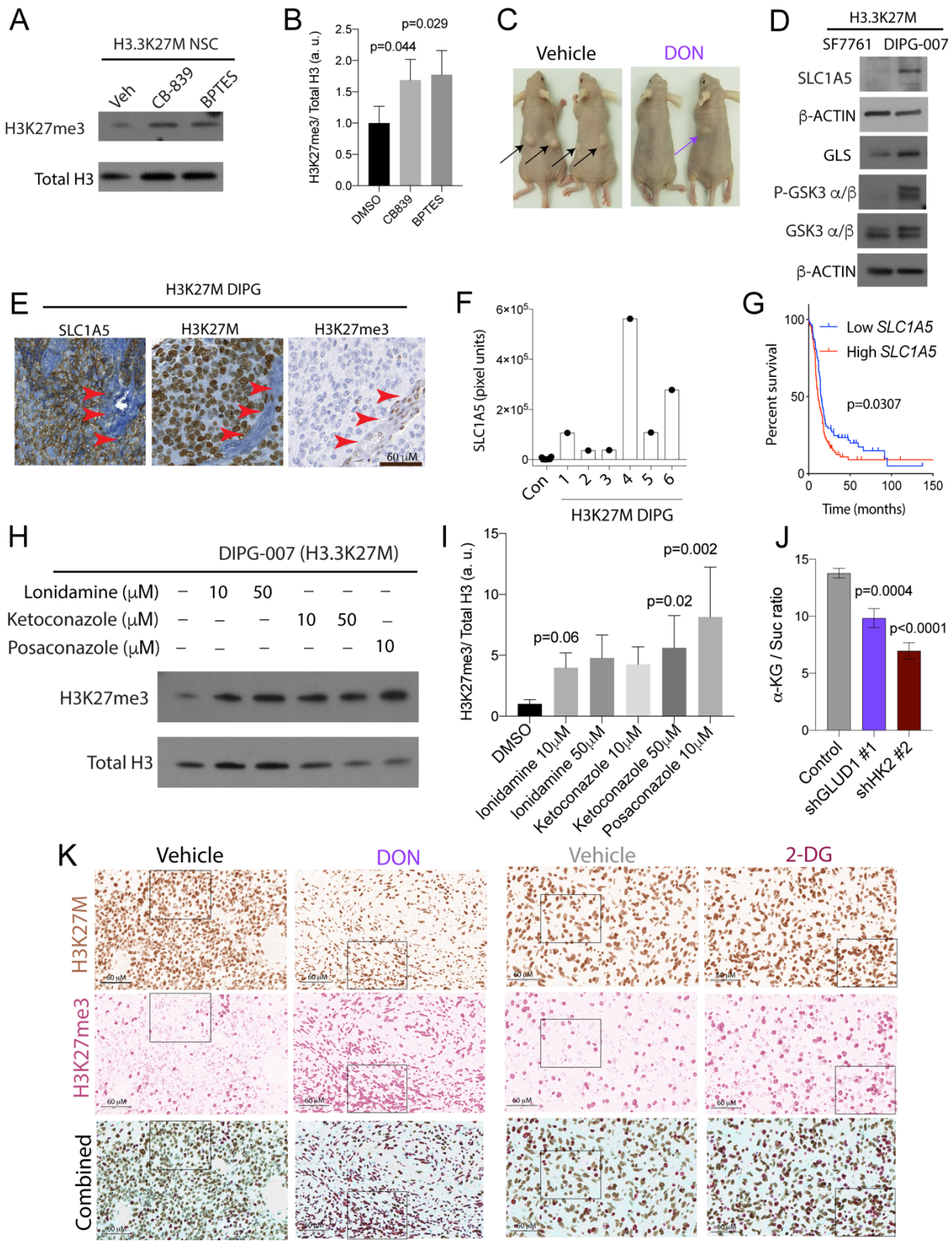
A
H3.3K27M NSC
Veh
CB-839
BPTES
H3K27me3
Total H3
B
p=0.029
p=0.044
H3K27me3/ Total H3 (a. u.)
DMSO
CB839
BPTES
C
Vehicle
DON
D
H3.3K27M
SF7761
DIPG-007
SLC1A5
β-ACTIN
GLS
P-GSK3 α/β
GSK3 α/β
β-ACTIN
E
H3K27M DIPG
SLC1A5
H3K27M
H3K27me3
60 μM
F
SLC1A5 (pixel units)
Con
H3K27M DIPG
G
Low SLC1A5
High SLC1A5
p=0.0307
Percent survival
Time (months)
H
DIPG-007 (H3.3K27M)
Lonidamine (μM)
Ketoconazole (μM)
Posaconazole (μM)
H3K27me3
Total H3
I
p=0.06
p=0.02
p=0.002
H3K27me3/ Total H3 (a. u.)
DMSO
Ionidamine 10μM
Ionidamine 50μM
Ketoconazole 10μM
Ketoconazole 50μM
Posaconazole 10μM
J
p=0.0004
p<0.0001
α-KG / Suc ratio
Control
shGLUD1 #1
shHK2 #2
K
Vehicle
DON
Vehicle
2-DG
H3K27M
H3K27me3
Combined

Figure S4. Inhibiting GDH and HK2 *in vitro* and *in vivo* increases global H3K27me3 levels and suppresses proliferation of H3.3K27M cells, related to figure 4

(**A-B**) H3.3K27M NSC were treated with vehicle (Veh) or the glutaminase inhibitors CB-839 (2μM) or bis-2-(5-phenylacetamido-1,3,4-thiadiazol-2-yl)ethyl sulfide (BPTES, 4μM) for 4 days. Representative WB of H3K27me3 and total H3 (**A**) and quantification normalized to total H3 (**B**) after treatment (n=3, each).

(**C**) Representative images from H3.3K27M NSC xenografted nude mice treated with vehicle or DON (1mg/kg, i.p., every other day for 6 weeks) from fig 4e. Arrows indicate tumors.

(**D**) Representative WB of SLC1A5, GLS, pGSK3 α/β, total GSK3 α/β and β-ACTIN in H3.3K27M- SF7761 and DIPG-007 cells.

(**E**) IHC for SLC1A5, mutant-specific H3K27M and H3K27me3 in consecutive sections of the same H3K27M DIPG tumor sample. Note SLC1A5 expression in H3K27M positive cells with reduced H3K27me3. Red arrows denote endothelial cells that are negative for SLC1A5 and H3K27M but retain H3K27me3 and serve as an internal control.

(**F**) Quantification for the glutamine transporter SLC1A5 in control brains (n=6) or H3.3K27M DIPG tumor samples (n=6, #1-6) from 4f.

(**G**) Log-rank analysis of overall survival in high-grade pediatric glioma patients stratified by high (above median, n=94) or low (below median, n=94) *SLC1A5* expression. Data derived from PedcBioPortal.

(**H-I**) DIPG-007 cells were treated with vehicle (Veh) or indicated concentrations (μM) of the HK2 inhibitors lonidamine, ketoconazole or posaconazole (Agnihotri et al., 2019) for 4 days. Representative WB of H3K27me3, and total H3 (**h**) and quantification normalized to total H3 (**i**) levels after treatment. Note that H3K27me3 increases on treatment with all three drugs compared to vehicle treated cells.

(**J**) Bar graph demonstrating α-KG/ suc ratios in H3.3K27M DIPG-007 cells with or without GLUD1 or HK2 knockdown (n=3, each).

(**K**) Corresponding low-power images of Figure 4m. Boxes indicate regions illustrated in Figure 4m.

Data plotted as mean ± SD and analyzed by ANOVA; n indicates biologic replicates.

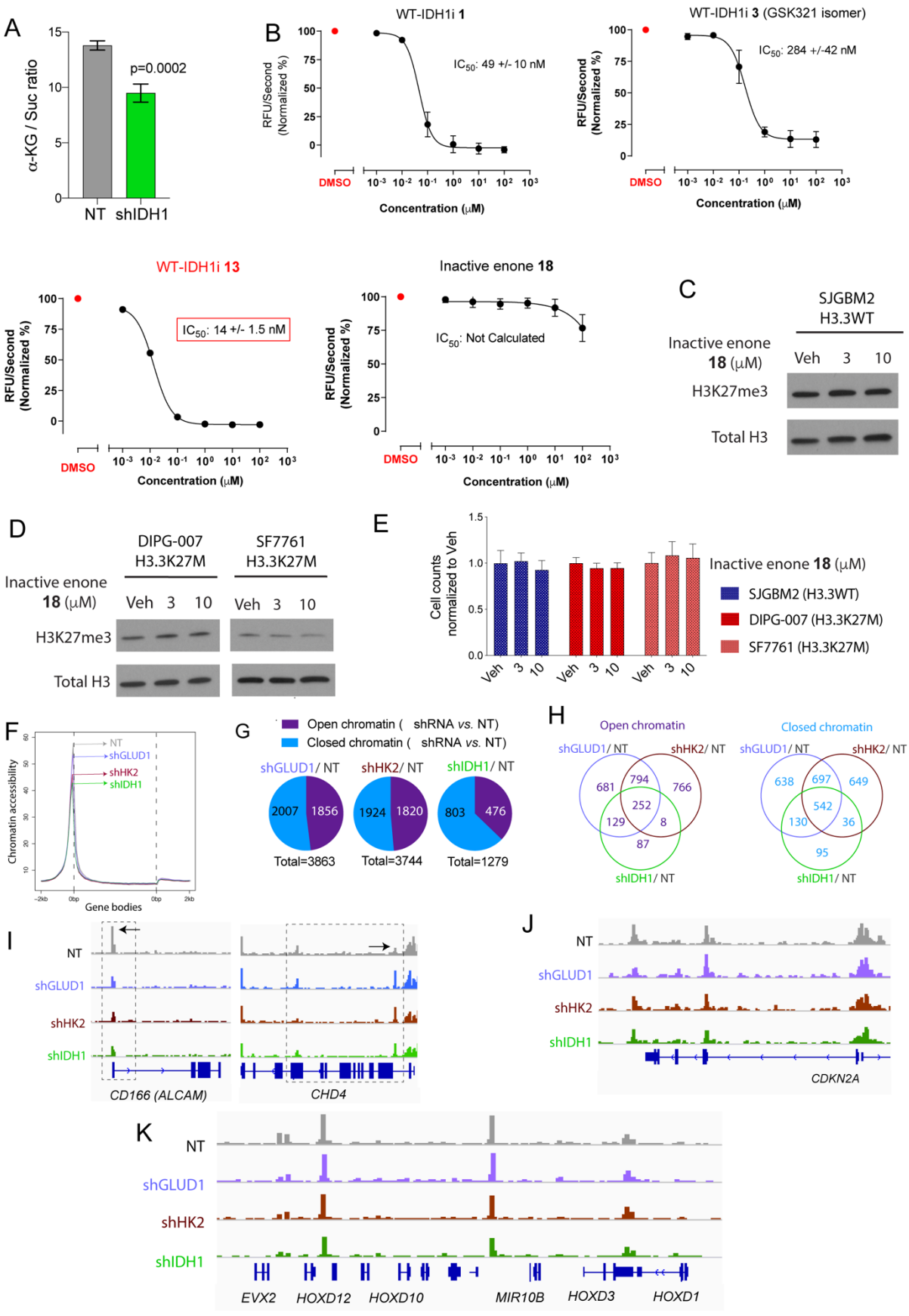
A
α-KG / Suc ratio
p=0.0002
NT
shIDH1
B
WT-IDH1i 1
RFU/Second (Normalized %)
IC50: 49 +/- 10 nM
DMSO
Concentration (μM)
WT-IDH1i 3 (GSK321 isomer)
IC50: 284 +/-42 nM
WT-IDH1i 13
IC50: 14 +/- 1.5 nM
Inactive enone 18
IC50: Not Calculated
C
SJGBM2
H3.3WT
Inactive enone 18 (μM)
Veh 3 10
H3K27me3
Total H3
D
DIPG-007
H3.3K27M
SF7761
H3.3K27M
E
Cell counts normalized to Veh
Inactive enone 18 (μM)
SJGBM2 (H3.3WT)
DIPG-007 (H3.3K27M)
SF7761 (H3.3K27M)
F
Chromatin accessibility
NT
shGLUD1
shHK2
shIDH1
Gene bodies
G
Open chromatin (shRNA vs. NT)
Closed chromatin (shRNA vs. NT)
shGLUD1/ NT
shHK2/ NT
shIDH1/ NT
2007
1856
1924
1820
803
476
Total=3863
Total=3744
Total=1279
H
Open chromatin
Closed chromatin
681
794
766
252
129
8
87
638
697
649
542
130
36
95
I
CD166 (ALCAM)
CHD4
J
CDKN2A
K
EVX2
HOXD12
HOXD10
MIR10B
HOXD3
HOXD1

Figure S5. Inhibiting IDH1 increases H3K27me3 levels and is toxic, and GDH, HK2 and IDH1 knockdown results in altered chromatin accessibility at gene loci related to neuroglial differentiation, related to figure 5

(**A**) Bar graph demonstrating α-KG/ suc ratios in H3.3K27M DIPG-007 cells with or without IDH1 knockdown (n=3, each).

(**B**) WT-IDH1 activity curves (measuring conversion of NAPD to NAPDH, relative florescence units/second; RFU/sec, Y-axis) plotted as a function of concentrations (μM, X-axis) using indicated active or inactive WT-IDH1 inhibitors. IC_{50} values for each compound are indicated. Note that compound **13** has the lowest IC_{50} value, while inactive enone analogue **18** does not inhibit WT-IDH1 enzymatic activity (n=3, each).

(**C-D**) H3WT (SJGBM2, **C**) or H3.3K27M (DIPG-007 and SF7761, **D**) were treated with vehicle (Veh) or indicated concentrations of the inactive enone analogue (compound **18**) for 2 days. WB of H3K27me3 and total H3 levels after treatment. In parallel, cell counts (Y-axis) was measured in each condition after 2-day treatment (**E**, n = 3, each).

(**F**) ATAC-seq was compared in DIPG-007 cells stably transduced with non-targeted (NT, dark gray) or shGLUD1 (light blue), shHK2 (brown) and shIDH1 (green). Chromatin accessibility was compared at gene body regions (n=2, replicates, each).

(**G-H**) Pie charts indicating number of regions with open chromatin (increased chromatin accessibility, significantly upregulated in shRNA/NT, purple) and closed chromatin (lowered chromatin accessibility, significantly downregulated in shRNA/NT, blue) in each shRNA condition (**G**) and Venn diagram indicating intersection of regions with open or closed chromatin (**H**) from all three shRNAs. Non-overlapping regions could represent inbuilt redundancies in glucose and glutamine pathways.

(**I**) Representative ATAC-seq peaks at *CD166/ALCAM* and *CHD4* loci in H3.3K27M DIPG-007 cells expressing NT (dark gray), shGLUD1 (light blue), shHK2 (brown) and shIDH1 (green) H3.3K27M DIPG-007 cells. Dotted boxes are regions indicated in Figure 5j and 5l.

(**J-K**) Representative ATAC-seq peaks at *CDKN2A* (**j**) and *EVX2, HOXD12, HOXD10, MIR10B, HOXD3, HOXD1* (**k**) loci in NT (dark gray), shGLUD1 (light blue), shHK2

(brown) and shIDH1 (green) H3.3K27M DIPG-007 cells. Note that no differences were noted at these loci known to normally retain H3K27me3 in H3K27M cells (Bender et al., 2013; Chan et al., 2013; Mohammad et al., 2017).

Data plotted as mean ± SD and analyzed by 2-sided, unpaired, 2-tailed, Student's t-test (S5a) or ANOVA (S5e); n indicates biologic replicates.

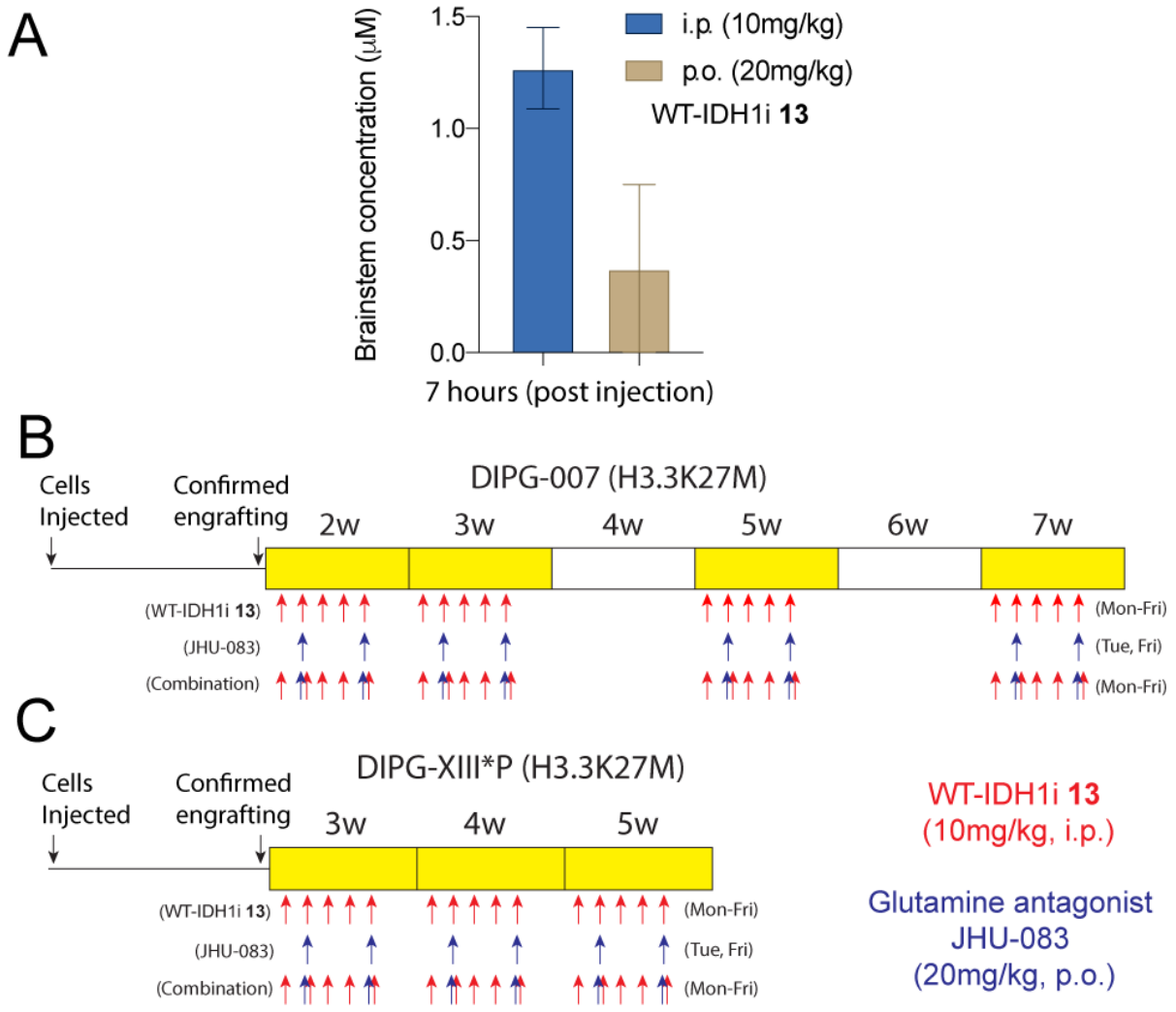

Figure S6. Inhibition of IDH1 and glutamine metabolism is therapeutic *in vivo,* related to figure 6

(**A**) Concentrations of IDH1 inhibitor **13** in the brainstem were determined in animals after i.p. injection of 10mg/kg or oral administration (p.o.; oral gavage) of 20mg/kg of the inhibitor. After seven hours, drug concentrations in the brainstem were measured using mass spectroscopy. Note that IDH1 inhibitor **13** reached higher brain concentrations on i.p. versus p.o. administration (n=3).

(**B-C**) Treatment regimens in animals orthotopically implanted with H3.3K27M DIPG-007 (**B**) and DIPG-XIII*P (**C**) cells (400,000 cells).

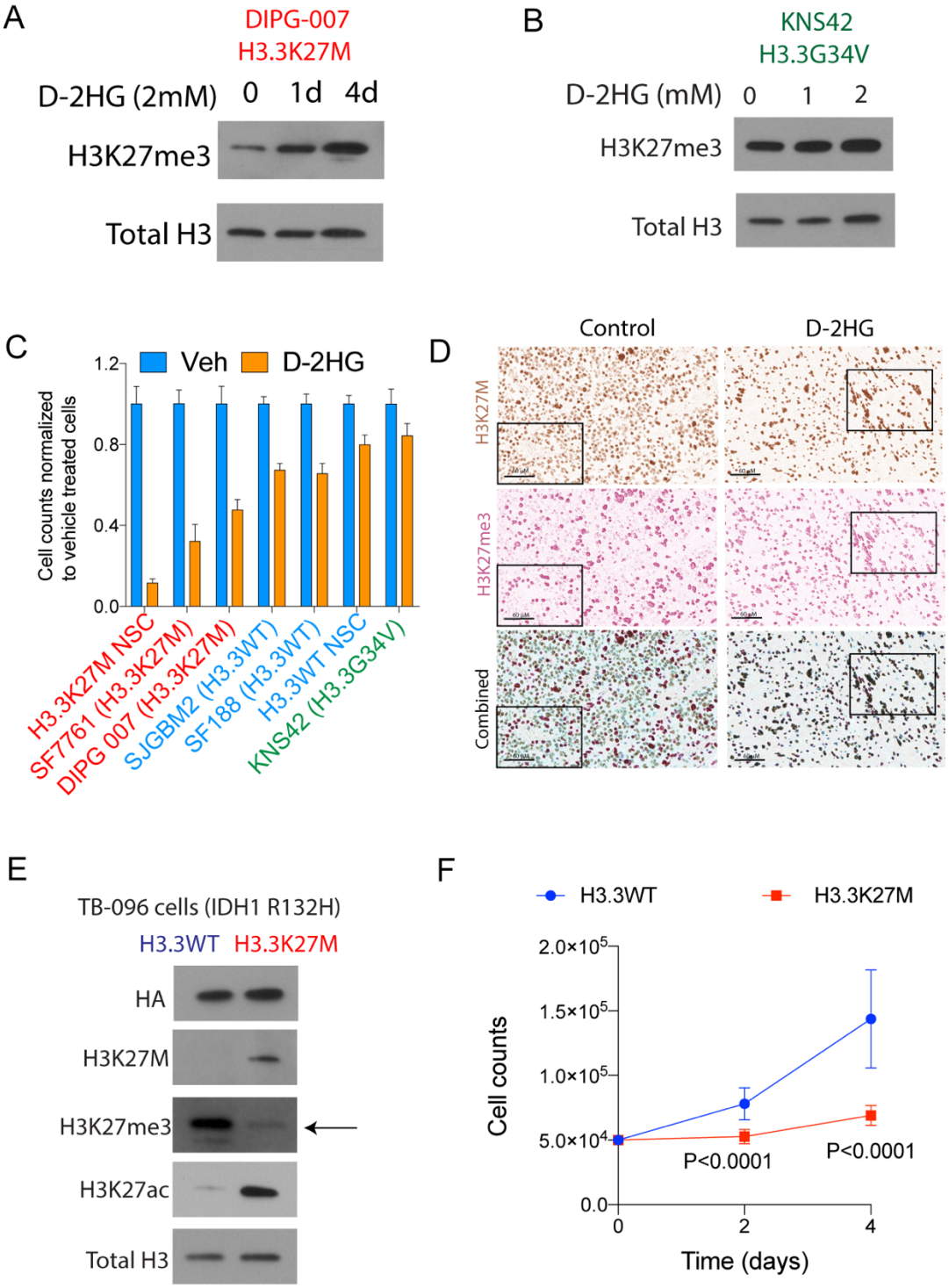
A
DIPG-007
H3.3K27M
D-2HG (2mM) 0 1d 4d
H3K27me3
Total H3
B
KNS42
H3.3G34V
D-2HG (mM) 0 1 2
H3K27me3
Total H3
C
Veh
D-2HG
Cell counts normalized to vehicle treated cells
1.2
0.8
0.4
0.0
H3.3K27M NSC
SF7761 (H3.3K27M)
DIPG 007 (H3.3K27M)
SJGBM2 (H3.3WT)
SF188 (H3.3WT)
H3.3WT NSC
KNS42 (H3.3G34V)
D
Control
D-2HG
H3K27M
H3K27me3
Combined
E
TB-096 cells (IDH1 R132H)
H3.3WT H3.3K27M
HA
H3K27M
H3K27me3
H3K27ac
Total H3
F
H3.3WT
H3.3K27M
Cell counts
2.0×10^5
1.5×10^5
1.0×10^5
5.0×10^4
0.0
P<0.0001
P<0.0001
0
2
4
Time (days)

Figure S7. D-2HG increases H3K27me3 levels and is toxic to H3.3K27M cells and mutually exclusive H3.3K27M and IDH1 R132H mutations are synthetic lethal, related to figure 7

(**A**) H3.3K27M DIPG-007 cells were treated with 2 mM of D-2HG for 1 or 4 days. Representative WB illustrating changes in H3K27me3 and total H3 levels after treatment in each condition.

(**B**) High-grade glioma cells with H3.3G34V mutations (KNS42, green) were treated with indicated concentrations of D-2HG for 1 day. Representative WB of H3K27me3 and total H3 levels after treatment in each condition.

(**C**) Cell numbers (normalized cell counts, Y-axis) were measured in vehicle (Veh, light blue) or D-2HG (1 mM, orange) treated H3.3K27M and H3WT cells (n=3) depicted in figure 7e-f.

(**D**) Corresponding low-power images of Figure 7g. Boxes indicate regions illustrated in Figure 7g.

(**E-F**) IDH1 R132H TB-096 glioma cells were stably transduced with H3.3WT (blue) or H3.3K27M (red). Representative WB of HA-tag, H3K27M, H3K27me3, H3K27ac and total H3 levels in each condition (**E**). Cell proliferation (cell counts, Y-axis) of cells plotted against time (days, X-axis) in each condition (**F**, n = 3).

Data plotted as mean ± SD and analyzed by 2-sided, unpaired, 2-tailed, Student's t-test, n indicates biologic replicates.